Journal of Alloys and Compounds 509 (2011) 9093–9097

Contents lists available at ScienceDirect

Journal of Alloys and Compounds

journal homepage: www.elsevier.com/locate/jallcom

Ultrasonic-assisted in situ synthesis and characterization of superparamagnetic Fe_3O_4 nanoparticles

Jie Feng, Jian Mao*, Xiaogang Wen, Mingjing Tu

College of Materials Science and Engineering, Sichuan University, Chengdu 610064, PR China

ARTICLE INFO

Article history:
Received 31 December 2010
Received in revised form 8 June 2011
Accepted 14 June 2011
Available online 7 July 2011

Keywords:
Superparamagnetism
Fe_3O_4 nanoparticles
Surfactant
Grain size
Saturation magnetization

ABSTRACT

Superparamagnetic Fe_3O_4 nanoparticles were synthesized via a modified coprecipitation method, and were characterized with X-ray diffraction (XRD), vibrating sample magnetometer (VSM), Zeta potential and FT-IR, respectively. The influences of different kinds of surfactants (sodium dodecyl benzene sulfonate, polyethyleneglycol, oleic acid and dextran), temperatures and pH values on the grain size and properties were also investigated. In this method, Fe^{3+} was used as the only Fe source and partially reduced to Fe^{2+} by the reducing agent with precise content. The following reaction between Fe^{3+}, Fe^{2+} and hydroxide radical brought pure Fe_3O_4 nanoparticles. The tiny fresh nanoparticles were coated in situ with surfactant under the action of sonication. Comparing with uncoated sample, the mean grain size and saturation magnetization of coated Fe_3O_4 nanoparticles decrease from 18.4 nm to 5.9–9.0 nm, and from 63.89 emu g^{-1} to 52–58 emu g^{-1} respectively. When oleic was used as the surfactant, the mean grain size of Fe_3O_4 nanoparticles firstly decreases with the increase of reaction temperature, but when the temperature is exceed to 80 °C, the continuous increase of temperature resulted in larger nanoparticles. the grain size decreases gradually with the increasing of pH values, and it remains unchanged when the PH value is up to 11. The saturation magnetization of as-prepared Fe_3O_4 nanoparticles always decreases with the fall of grain size.

1. Introduction

As a kind of important magnetic materials, superparamagnetic iron oxide nanoparticles can be widely used in many fields, such as cell separation, magnetic resonance imaging, ferrofluids, recording materials, chemical sensors, catalysis, magnetic targeted therapy and so on [1–6]. For future highly sensitive magnetic nanodevices and biological applications, iron oxide nanoparticles with controlled-shape, -size, and a narrow size distribution are urgent [7,8]. In recent years, investigations on preparation and application of nano-Fe_3O_4 crystal are receiving particular attention. For example, Zhang et al. [9] synthesized magnetite nanoparticles with improved magnetic properties by using sonochemistry method. Wang and co-workers [10] reported a preparation method for mesoporous Fe_3O_4 via citric acid-assisted solid thermal decomposition of ferric nitrate. Chen et al. [7] demonstrated the controlled synthesis of Fe_3O_4 nanosheets via one-step pyrolysis of EDTA ferric sodium salt. Among the numerous preparation methods, chemical coprecipitation process had the advantages of simple operation, low cost and mass production [11]. However, it also shared some flaws and deficiencies such as impurity of production, poor dispersity, and nonuniform particle size, and so on.In order to solve these problems, in this paper, firstly, Fe^{3+} was adopted as the only Fe source, the anhydrous sodium sulfite with the designed content was used to reduce Fe^{3+} to Fe^{2+} up to the needed content, so as to avoid the oxidation of Fe^{2+} when being directly added, which was the main reason to cause the impurity of Fe_3O_4 production. Secondly, sonication was adopted to keep the tiny Fe_3O_4 nanoparticles separately. Thirdly, the separated fresh nanoparticles were encapsulated in situ by surfactant immediately. The above methods could avoid the agglomeration and gained the uniform and fine Fe_3O_4 nanoparticles. Meanwhile, the influences of different kinds of surfactants, temperatures and pH values on the grain size and superparamagnetic performance of Fe_3O_4 nanoparticles were also investigated.

2. Experimental procedures

2.1. Preparation of samples

All reagents used in our experiments were analytically pure grade. A typical preparation process of Fe_3O_4 nanoparticles encapsulated with surfactant was carried out as follows: 5 g $FeCl_3{\cdot}6H_2O$ and 0.85 g Na_2SO_3 were dissolved in 50 mL deionized water which added suitable surfactant with vigorous stirring at 50 °C. In our investigations, sodium dodecyl benzene sulfonate (SDBS), polyethyleneglycol (PEG)-6000, oleic acid (OA) and dextran were used as the surfactant, respectively. Then 100 mL NaOH solution (0.8 mol L^{-1}) was injected into the above solution slowly with stirring at 1200 rpm by a mechanical stirrer, after finishing the addition of NaOH solution, kept the temperature at 80 °C for 60 min. During all the time, the reaction was under ultrasonic condition (40 KHz, 200 W). Finally, the magnetic nanoparticles

---

* Corresponding author.
E-mail address: maojianemail@163.com (J. Mao).

0925-8388/$ – see front matter © 2011 Elsevier B.V. All rights reserved.
doi:10.1016/j.jallcom.2011.06.053

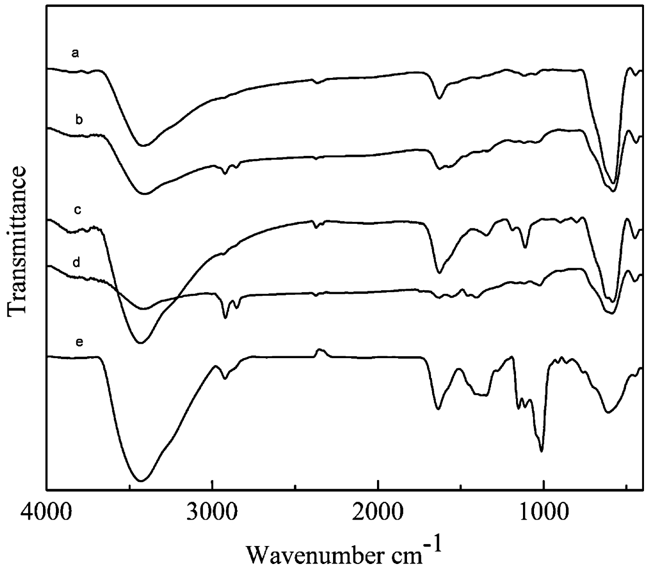

Fig. 1. FT-IR spectra of as-prepared nanoparticles without modification (a), with coatings of SDBS (b), PEG-6000 (c), oleic acid (d), and dextran (e), respectively.

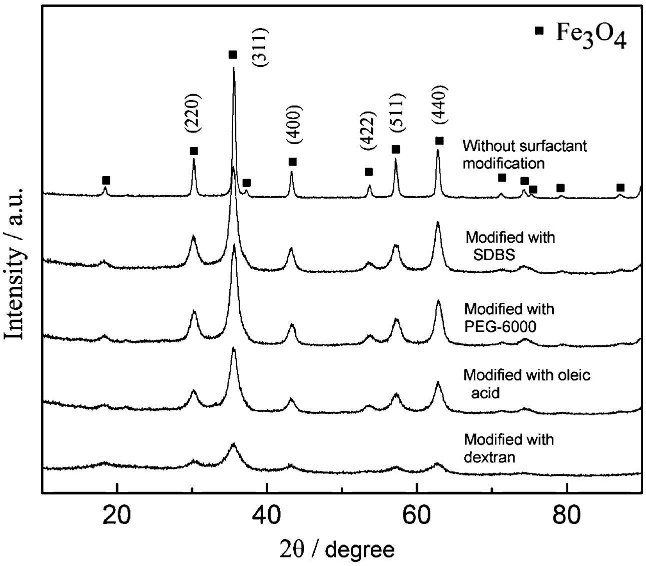

Fig. 2. XRD patterns of the as-prepared nanoparticles.

were isolated from the liquid by magnetic decantation and washed with deionized water and ethanol for several times, respectively. Then dried in a vacuum oven at 70 °C and stored in a desiccator for the next investigations.

2.2. Characterization

The as-prepared nanoparticles were characterized by a Rigaku Dmax-2000 X-ray diffractometer (Cu-Kα_1 = 0.154056 nm, 40 kV, 250 mA), and the mean grain size of sample was calculated with the Scherer's equation using X-ray diffraction (XRD) data. Lake Shore 7407 vibrating sample magnetometer (VSM) was used to measure the magnetic hysteresis loop. The Zeta potential of the magnetic nanoparticles was determined using Malvern Nano ZS90 apparatus at 25 °C. For the Zeta potential measurements, each sample was dispersed in deionized water by sonication. FT-IR measurements of nanoparticles were carried out with Bruker Tensor 27 Fourier transformed infrared spectrometer.

3. Results and discussion

3.1. Influence of surfactants on Fe_3O_4 nanoparticles

All the samples discussed in this section were prepared at the same conditions except surfactant: pH value was controlled by the same NaOH concentration; temperature was at 80 °C. Fig. 1 shows the FT-IR spectra of samples modified with surfactants. There are three obvious peaks at 3420 cm^{-1}, 1630 cm^{-1} and 580 cm^{-1} in the spectrum of all the synthesized nanoparticles. The first two peaks basically represent the vibrations of O–H stretching and H–O–H bending, respectively [12]. The last peak can be attributed to Fe–O stretch vibrations [13]. In the curve b, the characteristic peaks of SDBS at 1393 cm^{-1} and 1047 cm^{-1} can be assigned to bending vibration of C–H and stretching vibration of SO, respectively. In the curve c, C–O–C stretching vibration peaks of PEG is observed at 1111 cm^{-1} and 1161 cm^{-1}. The peaks at 1568 cm^{-1} and 1520 cm^{-1} in the curve d are the symmetric and asymmetric COO–stretch, respectively, which indicate that oleic acid was bonded to the surface of nanoparticles through covalent bond between COO– and Fe atom [14–16]. Curve e is the FT-IR spectroscopy of the nanoparticles modified with dextran, of which the peaks around 2922 cm^{-1} and 2852 cm^{-1} were regarded as the asymmetric and symmetric vibrations of C–H in –CH2–, respectively [17,18]. These FT-IR results imply that the nanoparticles were coated with the surfactants successfully.

Fig. 2 shows the XRD patterns of samples. The measured diffraction angles are consistent with those from the standard XRD patterns of magnetite (Fe_3O_4, JCPDS65-3107) with no extra peaks observed. In fact, the XRD pattern of magnetite (Fe_3O_4) is very similar with that of maghemite (γ-Fe_2O_3). In order to distinguish them, the difference between the lattice constant should be considered. Lattice constant '*a*' of magnetite (Fe_3O_4) and maghemite (γ-Fe_2O_3) was reported as 0.839 nm and 0.835 nm, respectively [19]. In our experiments, based on the six most intense peaks: (3 1 1), (4 4 0), (2 2 0), (5 1 1), (4 0 0) and (4 2 2) the calculated value of lattice constant 'a' of all the samples was about 0.838 nm–0.839 nm, it indicates that the phase is magnetite, not maghemite. The mean grain size of uncoated nanoparticles is 18.4 nm, and that of the coated samples are 9.0 nm, 7.4 nm, 6.4 nm and 5.9 nm for SDBS, PEG-6000, OA and dextran modification, respectively. The results indicate that the growth of grain could be restrained effectively by in situ covering treatment with surfactant under sonication. This could be attributed to the cavitation and thermal effect of ultrasound and the dispersing effect of surfactants. Compared with the pure Fe_3O_4 crystal spectra, the broadening of the peaks in the patterns of the modified Fe_3O_4 nanoparticles might be due to the decrease of grain size, the magnetization relaxation from superparamagnetism and the nonmagnetic layer covering the nanoparticles [20].

The magnetic hysteresis loops of as-prepared nanoparticles are shown in Fig. 3. From which all the nanoparticles with surfactant modification exhibit better superparamagnetic performance than that of uncoated nanoparticles. Because the remanence (Mr) value of uncoated sample is 1.456 emu g^{-1}; while, that of the other sample is less than 0.7 emu g^{-1}. This could be attributed to the fact that, the covered nanoparticles were so small that they might be considered to have a single magnetic domain [21]. However, the mean grain size of uncoated Fe_3O_4 nanoparticles was 18.4 nm, greater than the critical size for superparamagnetic determination of Fe_3O_4 nanoparticles, which was just about 15 nm [22,23]. The saturation magnetizations (Ms) of uncoated Fe_3O_4 nanoparticles is 63.89 emu g^{-1}, and that of the other sample is 57.38 emu g^{-1}, 54.43 emu g^{-1}, 52.29 emu g^{-1} and 19.08 emu g^{-1} for SDBS, PEG-6000, oleic acid and dextran modification, respectively. The Ms value of covered nanoparticles is lower than that of uncoated Fe_3O_4 nanoparticles, which might be attributed to the smaller crystalline size and a non-magnetic shell formed by the covering layer around the Fe_3O_4 nanoparticle [24]. From the above studies, the oleic acid modification could gain the second smallest grain size and a high Ms value, which had more usefulness and versatility than the other surfactant modification. So, in the next section, oleic acid modifica-

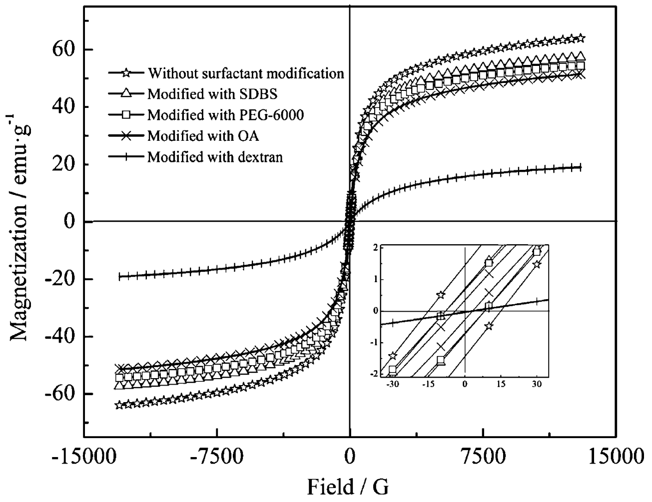

Fig. 3. Magnetic hysteresis loop of the as-prepared Fe_3O_4 nanoparticles, the inset is the enlargedview near the origin of coordinates.

tion was selected as the example to discuss the influence of reaction temperatures and pH value on the properties of nanoparticles.

Zeta potential as a function of pH values of the prepared Fe_3O_4 nanoparticles are shown in Fig. 4. The pH value at isoelectric point (pH_{IEP}) of the unmodified Fe_3O_4 nanoparticles was determined as about 6.4, that of Fe_3O_4 nanoparticles with PEG-6000 modification was determined as about 6.9 due to that PEG-6000 is non-ionic surfactants. The pH_{IEP} of the SDBS, OA and dextran modification Fe_3O_4 nanoparticles was determined as about 6.0, 6.2 and 4.2, respectively. Because the negative charged groups hydrolyzed from the SDBS, OA and dextran were around the Fe_3O_4 nanoparticles, which resulted in the pH_{IEP} of the three samples shifting to acid. The above Zeta potential results also indirectly proved that the success of cover treatment of Fe_3O_4 nanoparticles.

3.2. Influence of temperature on Fe_3O_4 nanoparticles

In this section and the following, Fe_3O_4 nanoparticles with oleic acid modification were choosed as the example to discuss the influence of reaction temperature and pH value on the properties of nanoparticles.

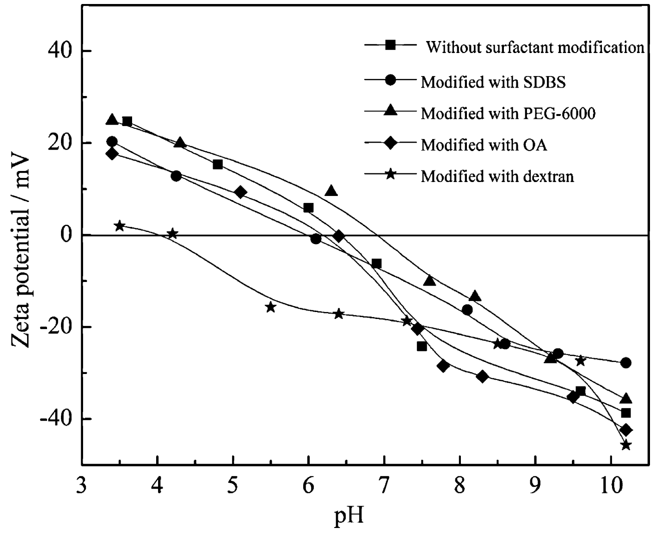

Fig. 4. Relationship between Zeta potential and pH values of prepared Fe_3O_4 nanoparticles.

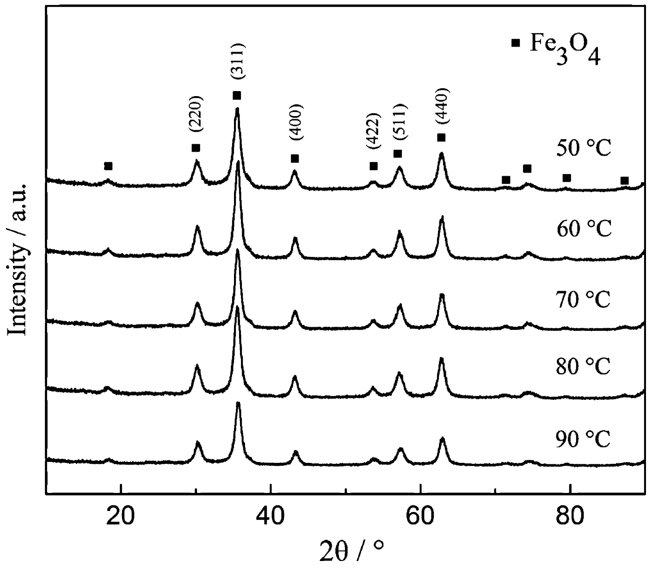

Fig. 5. XRD patterns of Fe_3O_4 nanoparticles with OA modification at various temperatures.

Fig. 5 shows the XRD patterns of Fe_3O_4 nanoparticles with oleic acid modification at various temperatures when the pH value was 11. The phase could be determined as magnetite Fe_3O_4 (JCPDS No. 65-3107) according to the XRD patterns. The mean grain size of sample is 7.9 nm, 7.3 nm, 7.2 nm, 6.0 nm and 6.9 nm, according to preparation temperature of 50 °C, 60 °C, 70 °C, 80 °C and 90 °C, respectively. It could be seen that the grain size of Fe_3O_4 nanoparticles firstly decreased with the increase of temperature, until the temperature was up to 80 °C, then it began to rise when the temperature was up to 90 °C. Because oleic acid could not cover the nanoparticles completely when the temperature was less than 80 °C, the uncoated part of nanoparticles could grow up freely. The degree of cover integrity increased gradually with the temperature rising, when it was up to 80 °C, oleic acid could cover the nanoparticles completely, which restrained the growth of crystallite grain successfully. When temperature was above 80 °C, oxidization of oleic acid could be found, which affected the covering effectiveness, so as to the growth of crystalline grain.

The magnetic hysteresis loop of Fe_3O_4 nanoparticles with oleic acid modification at various temperatures were shown in Fig. 6. It indicates that all the prepared nanoparticles possess superparamagnetic behavior. However, the Ms changes with the variation of

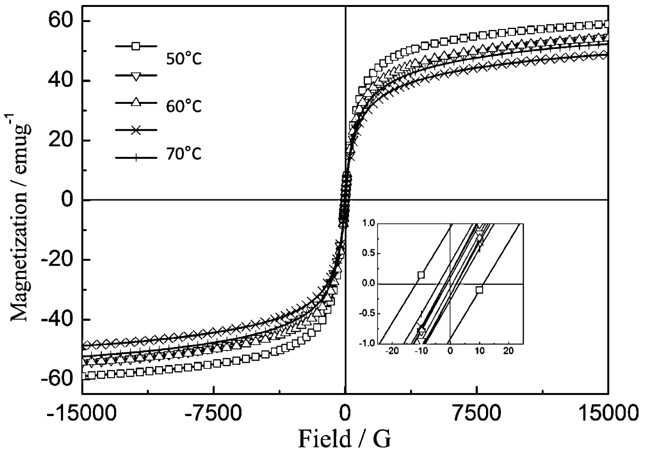

Fig. 6. Magnetic hysteresis loop of Fe_3O_4 nanoparticles with OA modification at various temperatures, the inset is the enlargedview near the origin of coordinates.

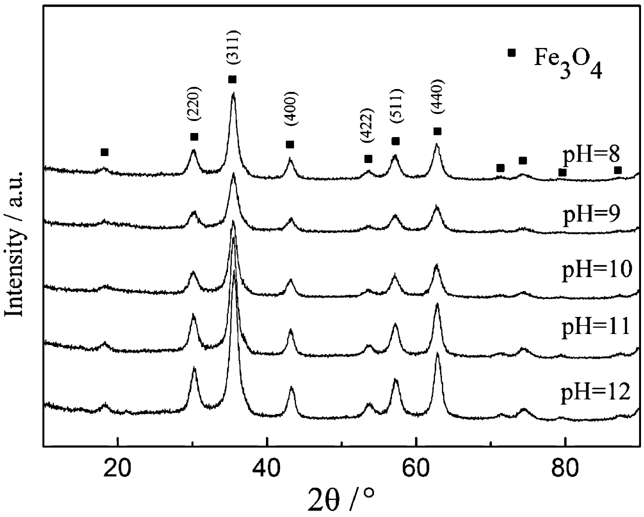

Fig. 7. XRD patterns of Fe_3O_4 nanoparticles with OA modification at various pH.

temperature. Firstly, Ms decreases with the increase of temperature, the value reached to the minimum when the temperature is 80 °C, then it increased with the increase of temperature which warmer than 80 °C. Considering the relationship between crystalline grain size and Ms, it seems that Ms of nanoparticles would increase with the increase of grain size.

3.3. *Influence of pH on Fe_3O_4 nanoparticles*

Fig. 7 shows the XRD patterns of Fe_3O_4 nanoparticles with oleic acid modification at various pH values when the temperature was 80 °C. These XRD patterns indicate that all sample are magnetite (JCPDS No. 65-3107). The mean grain size calculated with the Scherer's equation is 7.6 nm, 7.0 nm, 6.8 nm, 6.0 nm and 6.1 nm for pH value 8, 9, 10, 11 and 12, respectively. When pH value is less than 11, the grain size gradually decreases with the increase of pH values; while pH is over 11, the grain size remains unchanged nearly, because absolute value of Zeta potential of the Fe_3O_4 nanoparticles with oleic acid modification increases with the increase of pH (Fig. 4). Higher the absolute value of Zeta potential, better dispersibility of the nanoparticles. Which means that the fresh crystal grains formed from precipitation reaction are difficult to grow up depend on grain merging. When the pH value is over 11, the influence of pH increase on the dispersibility is not notable as that of lower pH, so that the grain size remains unchanged nearly.

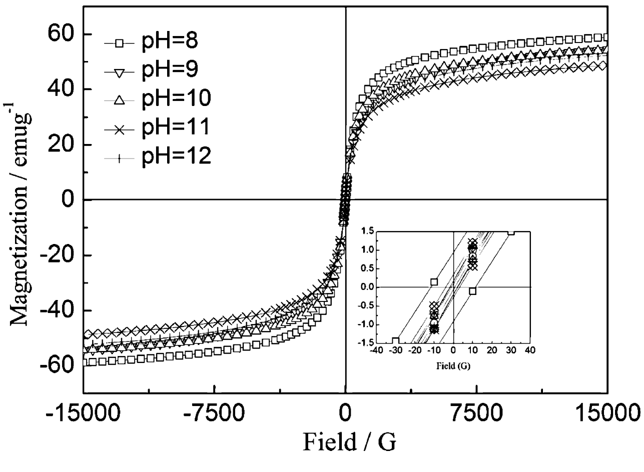

Fig. 8. Magnetic hysteresis loop of Fe_3O_4 nanoparticles with OA modification at various pH, the inset is the enlargedview near the origin of coordinates.

Fig. 8 shows the magnetic hysteresis loop of samples, in which the nanoparticles exhibit superparamagnetic behavior. When pH is less than 11, the saturated magnetization of Fe_3O_4 nanoparticles gradually decreases with the increase of pH values; while pH is over 11, the saturated magnetization basically keeps unchanged. The results indicate that the influence of grain size on the value of saturated magnetization is the same as that in Section 3.2.

4. Conclusions

(1) In the investigation, Fe^{3+} was adopted as the only Fe source and partially reduced to Fe^{2+} via adding reducing agent with precise content, the pure Fe_3O_4 crystal grains could be gained under the precipitation action of hydroxide radical. Then the fresh tiny nanoparticles formed from precipitation reaction were coated in situ with surfactant under the action of sonication. All the nanoparticles with surfactant modification exhibit better superparamagnetic performance than that of uncoated nanoparticles. Comparing to the uncoated sample, the mean crystal grain size of modified Fe_3O_4 nanoparticles decrease from 18.4 nm to 5.9–9.0 nm, and their saturation magnetization also decrease from 63.89 emu g^{-1} to about 52–58 emu g^{-1}, respectively.

(2) Using oleic acid as the surfactant, the mean grain size of Fe_3O_4 nanoparticles firstly decrease with the increasing reaction temperature until the temperature is up to 80 °C, and then begin to rise when the temperature increase. Because oleic acid could cover the nanoparticles completely only at 80 °C and restrain the growth of crystal grain successfully.

(3) Using oleic acid as the surfactant, the grain size of Fe_3O_4 nanoparticles gradually decrease with the increasing pH when it is less than 11; while pH value is over 11, the grain size remains unchanged. The mainly reason was the influence of the pH on the Zeta potential of nanoparticles, which could control the growth of crystal grain.

(4) In the investigations, decreasing of the crystallite size can reduce the saturation magnetization of as-prepared nanosized Fe_3O_4 samples.

Acknowledgments

This work was financially supported by National High Technology Research and Development Program of China (863 Program, no. 2007AA021801).

References

[1] G.F. Huang, J. Diakur, Z.H. Xu, Int. J. Pharm. 360 (2008) 197–203.
[2] C.L. Yang, J.M. X, Y.P. Guan, J.G. Liu, H.Z. Liu, J. Alloys Compd. 385 (2004) 283–287.
[3] R.Y. Hong, B. Feng, G. Liu, S. Wang, H.Z. Li, J.M. Ding, Y. Zheng, D.G. Wei, J. Alloys Compd. 476 (2009) 612–618.
[4] S.B. Ni, X.H. Wang, G. zhou, F. Yang, J.M. Wang, Q. Wang, D.Y. He, J. Alloys Compd. 505 (2010) 727–732.
[5] C. Ingrosso, M. Striccoli, A. Agostiano, E. Sardella, S. Keller, G. Blagoi, A. Boisen, M.L. Curri, Procedia Chem. 1 (2009) 32–35.
[6] I. Brigger, C. Dubernet, P. Couvreur, Adv. Drug Delivery Rev. 54 (2002) 631–651.
[7] L.Y. Chen, C.L. Zhao, Y. Zhou, H. Peng, Y.Y. Zheng, J. Alloys Compd. 504 (2010) L446.
[8] W.Z. Lv, B. Liu, Q. Qiu, F. Wang, Z. Luo, P.X. Zhang, S.H. Wei, J. Alloys Compd. 479 (2009) 480–483.
[9] X.P. Zhang, W.Q. Jiang, X.L. Gong, Z. Zhang, J. Alloys Compd. 507 (2010) 400–405.
[10] X.H. Liu, Y. Guo, Y.G. Wang, J.W. Ren, Y.Q. Wang, Y.L. Guo, Y. Guo, G.Z. Lu, Y.S. Wang, Z.G. Zhang, J. Mater. Sci. 45 (2010) 906–910.
[11] L.Q. Zhu, H. Zhang, W.P. Li, H.C. Liu, J. Alloys Compd. 471 (2009) 481–487.
[12] J. Giri, S.G. Thakurta, J. Bellare, A.K. Nigam, D. Bahadur, J. Magn. Magn. Mater. 293 (2005) 62–68.
[13] M. Arruebo, R. Fernandez-Pacheco, S. Irusta, J. Arbiol, M.R. Ibarra, J. Santamaria, Nanotechnology 17 (2006) 4057–4064.
[14] A.L. Willis, N.J. Turro, S. O'Brien, Chem. Mater. 17 (2005) 5970–5975.

[15] Y. Ren, K.I. Iimura, T. Kato, Langmuir 17 (2001) 26–88.
[16] Z. Li, L. Wei, M.Y. Gao, H. Lei, Adv. Mater. 17 (2005) 1001–1005.
[17] X.H. Sun, C.M. Zheng, F.X. Zhang, Y.L. Yang, G.G. Wu, A.M. Yu, N.J. Guan, J. Phys. Chem. C 113 (2009) 16002–16008.
[18] K.V.P.M. Shafi, A. Ulman, X.Z. Yan, N. Yang, C. Estournes, H. White, M. Rafailovich, Langmuir 17 (2001) 5093–5097.
[19] B. Tural, N. Özkan, M. Volkan, J. Phys. Chem. Solids 70 (2009) 860–866.
[20] Y.P. He, Y.M. Miao, C.R. Li, S.Q. Wang, L. Cao, S.S. Xie, G.Z. Yang, B.S. Zou, C. Burda, Phys. Rev. B 12 (2005) 5411–5416.
[21] X.Y. Qin, Nanostruct. Mater. 2 (1993) 99–106.
[22] J. Chatterjee, Y. Haik, C.J. Chen, J. Magn. Magn. Mater. 257 (2003) 113–118.
[23] S.E. Pratsinis, S. Vemury, Rev. Powder Technol. 88 (1996) 267–272.
[24] H.L. Ma, X.R. Qi, Yoshie Maitani, Tsuneji Nagai, Int. J. Pharm. 333 (2007) 177–186.